ELSEVIER

Polymer 44 (2003) 1499–1506

polymer

www.elsevier.com/locate/polymer

Physical gelation in ethylene–propylene copolymer melts induced by polyhedral oligomeric silsesquioxane (POSS) molecules

Bruce X. Fu[a], Michael Y. Gelfer[a], Benjamin S. Hsiao[a,*], Shawn Phillips[b], Brent Viers[b], Rusty Blanski[b], Patrick Ruth[b]

[a]*Department of Chemistry, State University of New York at Stony Brook, Stony Brook, NY 11794-3400, USA*
[b]*Propulsion Directorate, Air Force Research Laboratory, Edwards AFB, CA 93524-7680, USA*

Received 23 September 2002; received in revised form 9 December 2002; accepted 11 December 2002

Abstract

The rheological behavior of ethylene–propylene (EP) copolymers containing polyhedral oligomeric silsesquioxane (POSS) molecules was investigated by means of wide-angle X-ray diffraction (WAXD), oscillatory shear, stress and strain controlled rheology in the molten state and dynamic mechanical analysis (DMA) in the solid state. WAXD results showed that the majority of POSS molecules in the EP melt were present in the crystal form. Oscillatory shear results showed that the EP/POSS nanocomposites exhibited a solid-like rheological behavior compared with the liquid-like rheological behavior in the neat resin, i.e. POSS caused physical gelation in EP. While POSS exhibited only a minimum effect on the flow activation energy of EP, the high POSS concentration samples were found to induce higher yield stress than the neat resin. This behavior was similar to the Bingham rheology, indicative of a structured fluid. DMA results indicated that the presence of POSS increased the Young's modulus as well as the T_g of the EP copolymer. These results suggested that two types of interactions contributed to the physical gelation in EP/POSS melts were present: the strong particle-to-particle interactions between the POSS crystals and the weak particle-to-matrix interactions between the POSS crystals and the EP matrix.

Keywords: POSS; Ethylene–propylene copolymer; Nanocomposite

1. Introduction

Polymer nanocomposites—polymers filled with particles having at least one dimension in the nanometer range, have attracted tremendous attention from researchers in the field of polymer science during the recent years. Compared to neat polymers, nanocomposites can exhibit drastically improved mechanical and physical properties such as fire retardation performance even at relatively low concentrations of nanofillers. The cage-shaped polyhedral oligomeric silsesquioxane (POSS) molecules represent an emerging class of nanofillers. The chosen POSS system in this study has an empirical formula $(RSiO_{1.5})_8$, with R groups that can be chemically altered (a schematic drawing of this POSS is shown in Fig. 1). The POSS molecules can be incorporated into polymers (such as acrylics, polyamides and polyesters) by synthetic routes such as co-polymerization and chemical grafting or by physical mixing (in melt or in solution) [1–8]. In the current work, we have used the melt-mixing method to prepare the sample, since melt-mixing can be easily implemented in the industrial process.

POSS molecules differ from conventional fillers (e.g. carbon black) and other types of nanofillers (e.g. organoclay, carbon nanotube) in several aspects. POSS molecules can be dispersed in the polymer matrix at the level of individual molecules, which is much smaller in size (dimension ~15 Å) than the average dimension of conventional fillers. In contrast to other nanofillers, such as organoclay and carbon nanotubes, the shape of the POSS molecules is isotropic. The synthetic techniques for modification of the POSS molecules allow for the generation of a variety of functionalized substituents on the POSS cage [1–3,6]. This route creates an opportunity for fine-tuning the interactions between POSS molecules and polymer chains, and therefore provides ways to control the mechanical and rheological properties of nanocomposites. The relationships between the structures of POSS

* Corresponding author. Tel.: +1-631-632-7793; fax: +1-631-632-6518.
E-mail address: bhsiao@notes.cc.sunysb.edu (B.S. Hsiao).

0032-3861/03/$ - see front matter © 2003 Elsevier Science Ltd. All rights reserved.
doi:10.1016/S0032-3861(03)00018-1

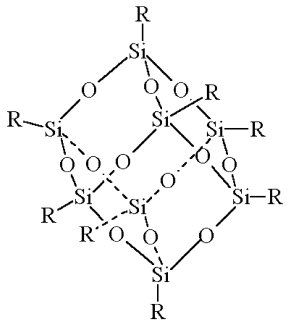

Fig. 1. Schematic diagram of octamethyl-POSS and octaisobutyl-POSS molecules.

molecules and of polymer matrix, and the resulting rheological and mechanical property changes in POSS nanocomposites have been investigated recently [4,5], yet some questions remain unanswered. For example, earlier studies showed that the introduction of POSS molecules chemically grafted to the polymeric chains results in the formation of a nanocomposite material having enhanced mechanical performance, higher glass transition temperature T_g and higher thermal decomposition temperature T_{dec}. Due to the absence of polar units in the POSS molecules used in the polystyrene (PS) matrix, it was proposed that most of the enhancements were caused by the retardation of polymer chains by POSS molecules. In other words, each individual POSS molecule, chemically linked to the PS oligomer can function as an 'anchor' point in the polymer matrix, and that the resulting PS/POSS polymer nanocomposite possesses a physical network with individual POSS molecules behaving as weak physical crosslinking sites [9]. It is not clear if this behavior exists in the physically blended POSS nanocomposites.

Compared to the chemically grafted POSS/polymer nanocomposites, relatively few researchers have studied physically blended POSS/polymer nanocomposites [10]. The physically blended POSS system has at least two features that are different from the chemically grafted POSS system: (1) there are no covalent POSS-polymer linkages, (2) the POSS molecules may aggregate and form crystals (the crystallization is often hindered in the chemically grafted systems). In the present work, we have used small-angle X-ray scattering (SAXS), wide-angle X-ray diffraction (WAXD), dynamic mechanical analysis (DMA), differential scanning calorimetry (DSC) and rheological techniques to investigate the POSS/polymer nanocomposites prepared by melt-mixing of ethylene-propylene (EP) copolymer with POSS molecules. The emphasis was made in two areas: (1) the relationship between the degree of POSS aggregation and the melt rheology of EP/POSS nanocomposites, and (2) the possible mechanism of physical gelation of EP matrix by POSS. The obtained DMA results indicated that the T_g of EP/POSS nanocomposites was higher than that of the neat resin, which was consistent with the formation of weak physical bonds between POSS and EP molecules.

2. Rheological approach to characterize physical gelation

The gelation process in polymers can be defined as the formation of a 3-D network where long-chain polymer molecules are bound by physical or chemical crosslinking. Due to the connectivity induced by the crosslinked points, the rheological behavior changes from melt-like to solid-like. The so-called 'gel point' separates the melt-like behavior from the solid-like behavior. From the rheological standpoint, the zero-shear rate viscosity and the longest relaxation time (λ) diverge as the system approaches the gel point, while the non-zero equilibrium shear modulus appears just beyond it. Based on the results from Winter et al., [12–14] the rheological behavior of a polymer at the gel point (critical gel) can be characterized by a so-called 'self-similar relaxation pattern'. The corresponding relaxation spectrum for a critical gel ($H(\lambda)$) can be expressed as [15],

$$H(\lambda) = \frac{S}{\Gamma(n)}\lambda^{-n} \qquad \text{for} \qquad \lambda_0 < t < \infty \tag{1}$$

where $\Gamma(n)$ is the gamma function, λ_0 represents the characteristic relaxation time of the transition from the rubbery plateau to the reptation regime in the low frequency zone or the 'terminal zone', S represents the gel stiffness (yield stress). The relaxation exponent n is between 0 and 1. Based on Eq. (1), the viscoelastic parameters for a critical gel can be rewritten to be [16],

$$G'_c(\omega) = \frac{G''_c(\omega)}{\tan(n\pi/2)} = S\Gamma(1-n)\cos(n\pi/2)\omega^n \qquad \text{for} \qquad 0 < \omega < 1/\lambda_0 \tag{2}$$

where ω is the angular frequency. At the critical gel point, the ratio between the loss and the storage moduli ($\tan\delta = G''/G'$) is frequency independent

$$\tan\delta_c = \frac{G''_c}{G'_c} = \tan\frac{n\pi}{2} \qquad \text{for} \qquad 0 < \omega < 1/\lambda_0 \tag{3}$$

or,

$$n = \frac{2\delta_c}{\pi} \qquad \text{for} \qquad 0 < \omega < 1/\lambda_0 \tag{4}$$

These distinct characteristics of the critical gels provide us an easy tool for determination of the gel point using rheological methods. Based on Eq. (4) it can be seen that at the gel point, $\tan\delta$ is frequency independent, so the critical gel manifests itself by the appearance of zero-slope 'plateau' in the $\tan\delta$ curve. The slopes in the $\tan\delta$ curves are negative for the melts and positive for the solids (gels) beyond the gel point. This creates an opportunity for the

rheological identification of melt–gel transition in nanocomposites.

3. Experimental

3.1. Sample preparation

Two ethylene–propylene (EP1 and EP2) copolymers having different ethylene contents were used in this study (shown in Table 1). The EP1 sample contained 59 wt% of ethylene co-monomer, and the ethylene content in EP2 was 48 wt%. Both samples exhibited very little crystallinity and were rubbery at room temperature. These samples were experimental materials provided by ExxonMobil Chemical Company, using the metallocene catalyst technology. The molecular weight and polydispersity of the polymers were determined by gel permeation chromatography (GPC). The melting temperature and the crystallinity of samples were estimated by means of differential scanning calorimetry (DSC). The two POSS molecules chosen: ((1) octamethyl-POSS ($C_8H_{24}O_{12}Si_8$) and (2) octaisobutyl-POSS ($C_{32}H_{72}O_{12}Si_8$)) were obtained from Hybrid Plastics, Inc. (Fountain Valley, CA) and were used as received. The molecular weights of octamethyl-POSS and octaisobutyl-POSS are 537 and 874 g/mol, respectively. EP/POSS nanocomposites were prepared by melt-mixing in a twin-screw micro-compounder (DACA Instrument). Table 2 lists the composition and the processing parameters of EP/POSS nanocomposites. The mixing was carried out at temperatures of 140 °C for EP1 and of 120 °C for EP2 using the rotation speed of 100 rpm for 15 min.

3.2. WAXD and SAXS

The WAXD and SAXS measurements were performed at the X27C Beamline in the National Synchrotron Light Source, Brookhaven National Laboratory. The wavelength of X-ray used was 0.137 nm. The sample-to-detector distances were 800 mm for SAXS and 93 mm for WAXD. A MAR CCD X-ray detector having a resolution of 1026 × 1026 pixels (pixel size = 157 μm) was used to collect 2-dimensional patterns. The SAXS patterns were calibrated with silver behenate, and the WAXD patterns were calibrated with the Al_2O_3 standard. The typical image acquisition time was 1 min.

Table 2
Composition and processing parameters of EP/POSS nanocomposites

Sample ID	POSS wt%	POSS type	Melt-blending temperature (°C)
EP1_00	0	Octamethyl-POSS	140
EP1_10	10	Octamethyl-POSS	140
EP1_20	20	Octamethyl-POSS	140
EP1_30	30	Octamethyl-POSS	140
EP1_B_20	20	Octaisobutyl-POSS	140
EP2_00	0	Octamethyl-POSS	120
EP2_20	20	Octamethyl-POSS	120

3.3. Rheological techniques

Small-amplitude oscillatory shear (SAOS) experiments were performed on a strain-controlled rheometer RMS-605E (Rheometrics Scientific, US, NJ) using the parallel plate set-up (the plate diameter was 25 mm). The sample was first held at 180 °C for 15 min to eliminate the effect of thermal history, and then subsequently cooled to the experimental temperatures. Measurements were performed in the temperature range of 120–200 °C and the frequency range of $0.1 < \omega < 100$ rad/s. The same strain amplitude $\gamma_a = 8\%$ was used in all oscillatory shear experiments. All tests were carried out under a nitrogen flow to avoid thermal decomposition. Yield stress measurements were performed using a stress-controlled rheometer (the High Resolution Model of STRESSTECH rheometer made by ATS Rheo-Systems, Inc.). This instrument was also equipped with the parallel plate fixtures (diameter = 25 mm).

3.4. DMA

A dynamic mechanical analyzer (Rheometrics RSA II) operated in a tensile mode was used to study the thermal mechanical properties of EP/POSS nanocomposites in the solid state. Samples were made in the form of rectangular strips having dimensions of $20 \times 5 \times 0.2$ mm^3. After clamping the sample to finger tightness (about 10 mN/m of torque), a constant tensile force of 0.1 N was applied to the sample. The experiment was performed at 1 Hz with a stretching ratio of 0.1%. The sample was first cooled to −80 °C then heated to near the melting temperature at a 5 °C/min rate.

Table 1
Composition and molecular weight information of ethylene–propylene copolymers

Sample ID	Ethylene content (wt%)	M_w	M_n	Melting temperature (°C)	Crystallinity
EP1	59	108,000	79,000	~120	~5%
EP2	48	153,000	74,000	~80	<2%

4. Results

4.1. Wide-angle X-ray diffraction

Fig. 2A shows the WAXD profiles of octamethyl-POSS at 26, 160, 180, and 200 °C, respectively. The linear intensity profiles were obtained by using an azimuthal scan from the circular averaging of the two-dimensional WAXD patterns. As seen, octamethyl-POSS shows distinct colloid crystal reflection peaks, whose positions and intensities do not change at temperatures below 200 °C. Both crystal structures of octamethyl-POSS and octaisobutyl-POSS have been reported to be triclinic according to the work of Barry et al. [11] Our X-ray results on POSS peak positions are in good agreement with Barry et al. Fig. 2B shows temperature dependence of WAXD profiles of the nanocomposite sample EP1_10 (10 wt% octamethyl-POSS in EP1). Distinct POSS crystal reflection peaks, whose positions were identical to those observed in pure octamethyl-POSS, were also seen. This indicated that the majority of POSS molecules in EP1_10 were in the form of crystals and they were stable over the entire range of tested temperatures. The widths of these peaks were relatively narrow. The width of the strongest reflection ($2\theta \sim 11°$) was used to estimate the average crystal size, which was in the range of 50 nm (using the Scherrer equation). This indicated that that the POSS colloid crystals were formed in nanoscale (or nanocrystals) in the composites. The POSS crystal reflection peaks persisted even when sample EP1_10 was in the molten state (note that the melting temperature of EP1_10 was about 140 °C). Another interesting observation was that the amorphous peak of EP was shifted to a lower angle at temperatures of 160, 180, and 200 °C, which could be attributed to the thermal expansion of the EP matrix.

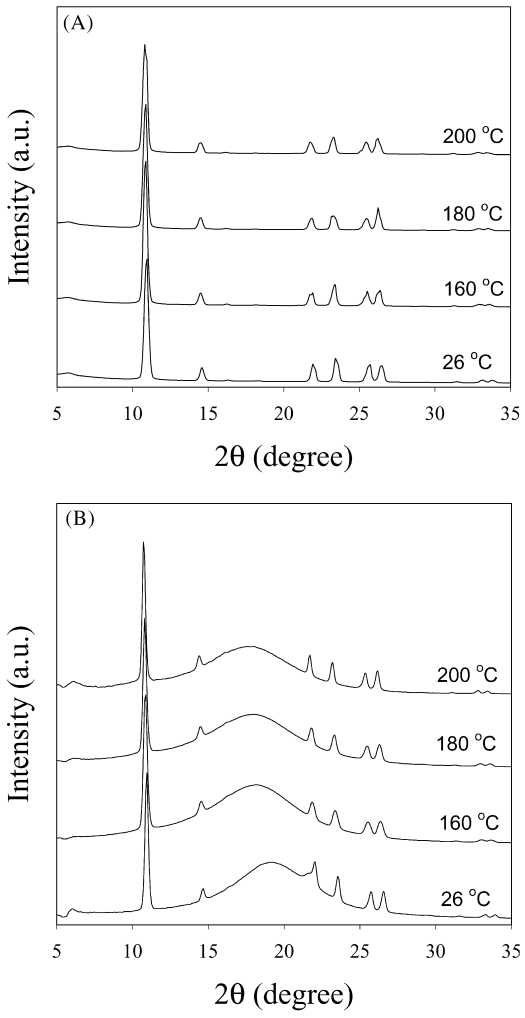

Fig. 2. WAXD profiles of (A) octamethyl-POSS and (B) EP1_10 (10 wt% octamethyl-POSS) at 26, 160, 180 and 200 °C after an azimuthal scan from collected two-dimensional WAXD patterns.

4.2. Dynamic mechanical analysis

The values of E' (Young's modulus) and tan δ from the DMA study of sample EP1_10 (10 wt% octamethyl-POSS) and sample EP1_00 (pure resin) are shown in Fig. 3. The addition of 10 wt% of octamethyl-POSS was found to result in a considerable increase of the Young's modulus (Fig. 3A). In the temperature region from −80 to 60 °C, the Young's modulus of the sample EP1_10 was about 1.7 times greater than that of EP1_00. As the temperature

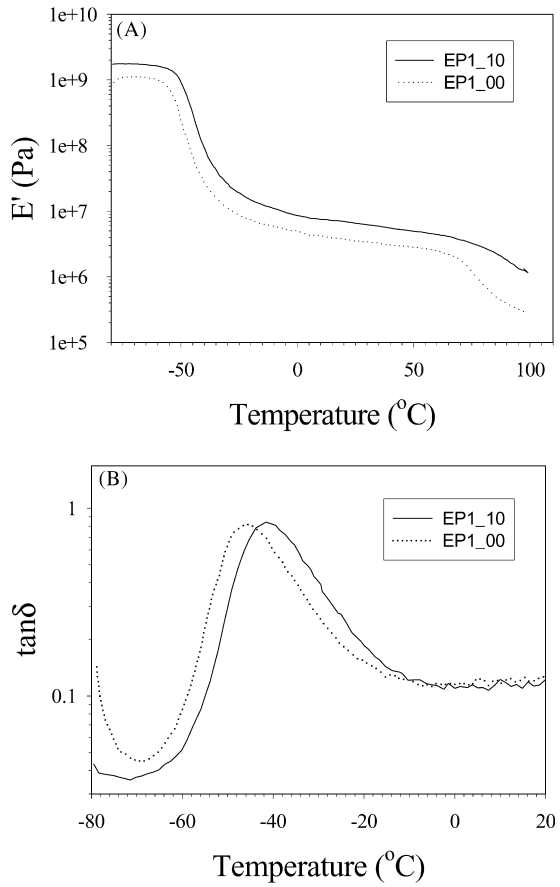

Fig. 3. An example of (A) Young's modulus and (B) tan δ changes of EP/POSS nanocomposite in a DMA temperature scan.

approached the melting point of EP1 (140 °C), the gap between the Young's moduli of the samples EP1_10 and EP1_00 increased. For example, at the temperature of 100 °C, the Young's modulus of the sample EP1_10 was about 5 times greater than that of EP1_00. The position of a peak maximum in the tan δ versus temperature curve can be related to the glass transition temperature (T_g). It was seen that the addition of 10 wt% octamethyl-POSS shifted T_g of EP towards a higher value by about 4.5 °C (Fig. 3B). This result suggested that the presence of POSS molecules resulted in a decrease of molecular mobility in EP either due to the induced constrains of the EP chains, or due to enhanced van der Waals bonding forces between POSS and the EP chains. In other words, the POSS nanocrystals exhibited some physical interactions with the EP polymer chains, which behavior has also been found in other POSS/polymer nanocomposites [1,5].

4.3. Small-angle X-ray scattering

The linear SAXS profiles of EP/POSS nanocomposites at different temperatures are shown in Fig. 4. As seen in Fig. 4A, pure EP exhibits a weak scattering peak at $q = 1.28\ \mathrm{nm}^{-1}$ (q is the scattering vector, $= 4\pi\sin\theta/\lambda$, where λ is the wavelength, 2θ is the scattering angle). This indicated that the EP copolymer had a lamellar structure even with a low degree of crystallinity (approximately 5% as determined by DSC). Upon heating to 160 °C, the sample was melted and the lamellar structure was destroyed. However, after cooling the above sample to 30 °C, the sample again showed the lamellar scattering peak at $q = 1.28\ \mathrm{nm}^{-1}$. The peak formed during cooling was rather sharp, indicating a well-defined lamellar structure. A similar phenomenon was also observed in the sample EP1_10 (Fig. 4B). In contrast, the sample EP1_30 (30 wt% octamethyl-POSS) showed a very ill-defined lamellar peak at 30 °C and after being cooled down to 30 °C from the melting temperature (Fig. 4C), which indicated that at high POSS content, the formation of the crystalline lamellae was hindered.

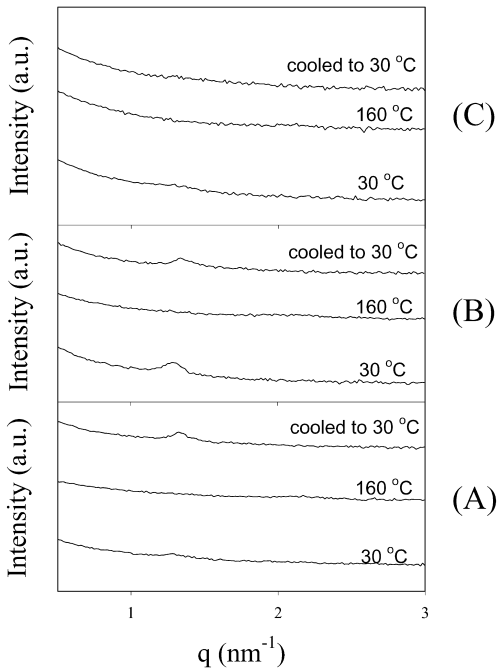

Fig. 4. SAXS profiles of samples (A) EP1_00; (B) EP1_10; (C) EP1_30 at 30, 160 °C and again 30 °C after being cooled down from 180 °C.

4.4. Oscillatory shear results

Fig. 5 shows the tan δ vs. ω plots for EP/POSS nanocomposites at 160 °C. It was seen that the rheological behavior of neat EP resin was typical of polymer melts having a negative slope in tan δ over the entire tested frequency range. The introduction of POSS molecules, however, drastically changed the EP1 rheology. In EP/POSS nanocomposites, the tan δ slope became positive in the low frequency region ($0.1 < \omega < 5$ rad/s). Based on the work by Winter et al., [12–16] these changes indicated the rheological transition from melt-like to solid-like (i.e. physical gelation). These data in Fig. 5 suggest that the gel point in EP/POSS nanocomposites is located at the POSS concentration (ϕ) between 0 and 10 wt%, where the tan δ slope in the terminal zone was frequency independent (a hypothesized dotted line was illustrated for the gel point in Fig. 5). The solid-like behavior in EP/POSS nanocomposites was also observed at higher temperatures (140, 180 and 200 °C) in EP/POSS nanocomposites at all POSS contents tested. The maximum in the tan δ curves was found to shift towards a higher frequency as the POSS concentration was increased, indicating the densification of the physically crosslinked network.

To further understand the effect of POSS on the viscoelastic properties of EP co-polymers, the relationship between the POSS concentration and frequency dependence of the storage modulus (G') is shown in Fig. 6. It was seen that at high frequencies the G' values were independent of POSS concentration, with the exception of EP1_30 showing a slightly higher G' value than those in EP/POSS nanocomposites and

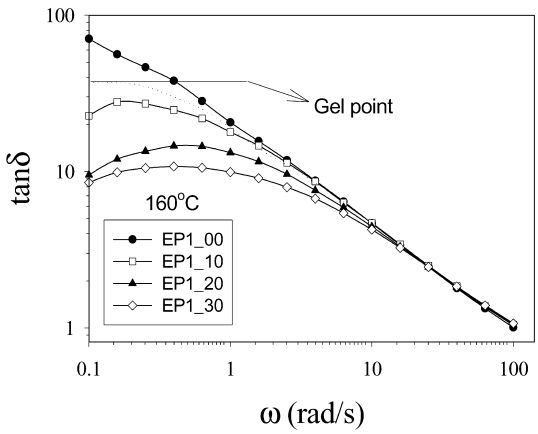

Fig. 5. tan δ value vs. ω for EP/POSS nanocomposites at 160 °C. The hypothesized dotted line represents the gel point.

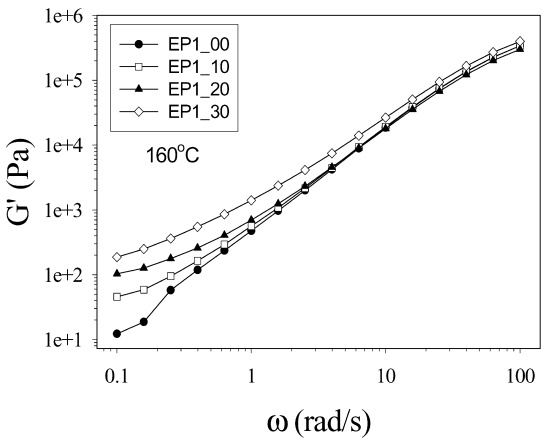

Fig. 6. Storage modulus (G') vs. ω for EP/POSS nanocomposites at 160 °C.

pure EP. Thus, the frequency dependence of the relaxation behavior in the high frequency region in EP/POSS nanocomposites was essentially unaffected by the addition of POSS molecules. In contrast, in the low frequency region, the slope of G' dependence in EP/POSS nanocomposites was lower than that in pure EP. The apparent plateau in G' at low frequencies observed in all EP/POSS nanocomposites was consistent with the solid-like viscoelastic behavior. A similar rheological response at the low frequency zone has also been observed in clay nanocomposites [17], fumed silica composites [18], and some polymer systems filled with large conventional fillers [19,20].

While the bulk of the present investigation focused on the POSS/polymer nanocomposites using the EP1 matrix, a POSS/polymer nanocomposite with EP2 was also tested. Fig. 7 shows two selected tan δ curves for the EP2/POSS nanocomposites at 120 °C. A similar transition from the typical melt-like behavior in the EP2_00 (neat resin) to the solid-like behavior in the EP2_20 (20 wt% octamethyl-POSS) was observed, which indicated that the gelation behavior also occurred in almost purely amorphous EP matrix (note that EP2 had a degree of crystallinity less than 2%). The effect of POSS structure on the gelation behavior in EP was also investigated.

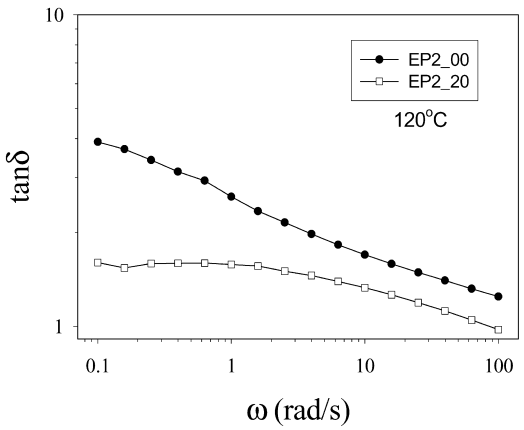

Fig. 7. tan δ value vs. ω for EP/POSS nanocomposite using pure EP2 as neat resin at 120 °C.

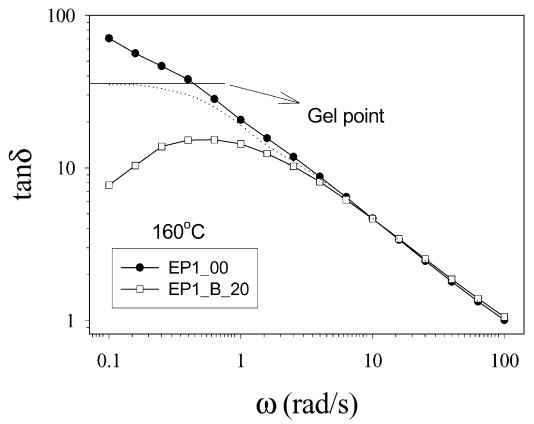

Fig. 8. tan δ value vs. ω for EP1/POSS nanocomposite containing 20 wt% octaisobutyl-POSS molecules at 160 °C. The hypothesized dotted line represents the gel point.

Fig. 8 shows two selected tan δ curves for the EP1/POSS nanocomposite containing 20 wt% octaisobutyl-POSS at 160 °C. Again, a similar transition from the typical melt-like behavior in EP1_00 (neat resin) to the solid-like behavior in EP1_B_20 (20 wt% octaisobutyl-POSS) was observed, which indicated that the gelation behavior was mainly related to the presence of the POSS nanocrystals in the polymer matrix rather than to the fine details of the POSS structure.

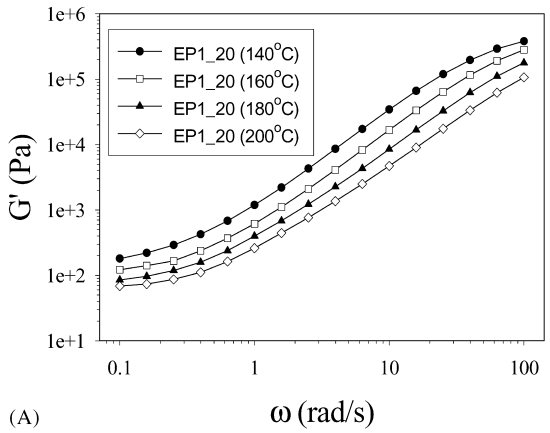

(A)

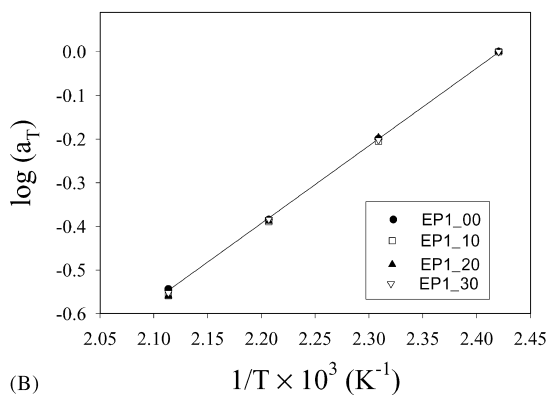

(B)

Fig. 9. (A) An example of the temperature effect on the storage modulus (G') in EP/POSS nanocomposites. (B) Frequency shift factors (a_T) as a function of temperature in EP/POSS nanocomposites.

Fig. 9A shows selected G' vs. ω profiles for sample EP1_20 at 140, 160, 180 and 200 °C, respectively. It was seen that the thermo-rheological behavior of EP/POSS nanocomposites obeyed the time-temperature superposition (TTS) principle—both G' and G'' master curves could be obtained by horizontally shifting along the ω axis. As seen in Fig. 9B, the frequency shift factors (a_T) of all the EP/POSS nanocomposites appear to be practically independent of POSS concentration. This indicated that the temperature-dependent relaxation processes observed in this particular viscoelastic measurement were essentially unaffected by the presence of the POSS molecules. In other words, the temperature dependent relaxation being probed was that of the polymer segments. These polymer segments were not confined by the POSS nanocrystals or bound to the POSS molecules significantly enough to affect the character of temperature dependence of the viscoelastic properties. Furthermore, almost constant flow activation energy was obtained in the EP/POSS nanocomposites. This flow activation energy was calculated by fitting the shift factor versus the temperature data with the Arrhenius equation, which was estimated to be around 34 kJ/mol for both neat EP resin and EP/POSS nanocomposites.

4.5. Yield stress measurements

The shear rate ($\dot{\gamma}$) vs. shear stress (τ) profiles measured using stress-controlled rheometer are illustrated in Fig. 10. It was seen that samples exhibited a Bingham-type rheological behavior with yield stress increasing with the increase in POSS concentration. Similar behavior was also observed at 140, 160, and 200 °C, respectively. It was found that the yield stress of the sample EP1_10 was very low at all temperatures. As POSS concentration increased, the yield stress values significantly increased. The onset of the yield stress was consistent with the solid-like rheology observed in the dynamic measurements. These observations suggest that the Bingham rheology observed in controlled stress experiments may be related to the breaking of aggregates of

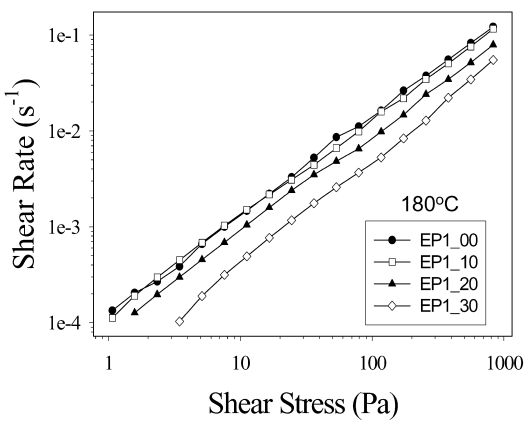

Fig. 10. Shear stress vs. shear rate for EP/POSS nanocomposites at 180 °C in stress-controlled rheological measurement.

POSS nanocrystals. Relatively low values of yield stress suggest that structures are rather weak, which is consistent with the notion that aggregation of non-polar POSS nanocrystals rather than EP/POSS binding is the major reason behind the observed solid-like rheological behavior.

5. Discussion

The stable thermodynamic approach developed by Leonov [21] has been widely applied by researchers for studying the rheology of filled polymers. This approach can successfully describe yielding, thixotropy and other rheological effects in a system where the particle-matrix interactions are much weaker than the interparticle interactions. However, it was found by some other researchers [22–24] that, in some filled systems, the particle-matrix interactions might be more important. An interesting example is the carbon black filled polymer system, which was found to be dominated by particle-matrix interactions. The major difference between the strong particle-to-particle interacting system and the strong particle-to-matrix interacting system is that the former yields at small deformations due to its short range interactions, and the latter yields at large deformations since the particles need to be debonded from the matrix. Rather low values of yield strain observed in our work suggest that the particle aggregation is a dominant factor to affect the rheological properties of EP/POSS nanocomposites. However, the polymer-filler interactions may also contribute to the measured rheological responses, as the WAXD results indicated the presence of significant amounts of POSS nanocrystals in the EP melt. It is conceivable that the fine dispersion of the POSS nanocrystals forms a 3-dimensional network, resulting in a solid-like rheological behavior that is often observed in concentrated suspensions. On the other hand, the increase in T_g of EP after the addition of POSS molecules observed *via* DMA suggests that the POSS nanocrystals may form some degrees of physical bonds with the polymer chains, resulting in a decreased chain mobility. Since high concentrations of POSS were used in this work, the cumulative weak interactions between the EP chains and the POSS nanocrystals may be sufficiently large to contribute to the solid-like rheological responses. Meanwhile, the confinement of some EP chains by densely dispersed POSS nanocrystals may also contribute to the increase in T_g. We suggest that the dominant factor causing the solid-like rheological behavior in the tested EP/POSS systems is the particle-to-particle interactions, while the weak particle-to-matrix interactions play a minor role. It should be noted that the solid-like rheology in POSS/polymer nanocomposites has been investigated before. For instance, Romo-Uribe et al [24] reported the drastic increase in the terminal relaxation time observed in the chemically grafted PS/POSS system, which was attributed to the 'sticky reptation' mechanism [25]. The authors suggested that the retardation of the polymer chain motion might come from the interchain interactions between the massive POSS molecules and the

polymer chains (PS). On the other hand, these authors also admitted that the sticky reptation mechanism could not be the sufficient explanation for a drastic change in the rheological behavior. In our case, the absence of chemical bonding between EP and POSS discounts the possibility of sticky reptations. The weak effect of POSS on the flow activation energy in the polymer matrix also indicates that the binding between the polymer matrix and POSS is very weak especially in the molten state. We propose that in nanocomposites containing chemically grafted molecules, the sticky reptations or the polymer-POSS interactions may play an important role. However in case of physical POSS/polymer blends, where the majority of POSS molecules form nanocrystals, the interactions between the adjacent POSS nanocrystals become dominant.

The possible dispersion of POSS molecules in the EP polymer matrix may include the following three scenarios. (1) The majority of POSS molecules exist in the form of nanocrystals, which are detectable by WAXD. (2) Some of the POSS nanocrystals can aggregate and form larger POSS crystal aggregates. The aggregation strength is relatively weak such that the aggregates can be broken apart by shear stress. (3) Some POSS molecules are dispersed at the molecular level. In cases (1) and (2), the particle-to-particle interactions are expected to dominate the rheology of the nanocomposite. However, in cases (1) and (3), some small POSS nanocrystals and molecularly dispersed POSS molecules can also interact with the polymer matrix by weaker bonding forces such as van der Waals forces.

6. Conclusions

In this study, we demonstrated that physical crosslinking in molten ethylene–propylene copolymers may be induced by addition of polyhedral oligomeric silsesquioxane (POSS) molecules. The small-amplitude oscillatory shear experiments showed that the presence of POSS molecules changed the rheological behavior above melting temperature from melt-like in the neat resin to solid-like in the nanocomposites. The frequency shift factors (a_T) at different temperatures were found to be independent of the POSS concentration, which indicated that thermorheological properties of EP were essentially unaffected by the POSS molecules. WAXD results showed formation of POSS crystal aggregates, suggesting that the particle-to-particle interactions between the POSS molecules contributed to the unusual rheological behaviors of the EP/POSS nanocomposites. The nanocomposite was observed to have higher T_g and higher Young's modulus than the neat resin, which suggested that the POSS nanocrystals formed weak bonds with polymer chains. SAXS results showed that at very high POSS concentration (30 wt%), the formation of EP crystal lamellar structures was hindered. The stress-controlled shear experiments showed that the introduction of POSS to the EP matrix increased the yield stress of EP.

Based on our results, we conclude that the physical gelation in the EP/POSS nanocomposite melt can be contributed to by two factors: the interactions between the POSS crystal aggregates (particle-to-particle), and the interactions between the POSS crystals and the polymer matrix (particle-to-matrix). We further postulate that the particle-to-particle interactions dominate the rheological behavior of physically mixed polymer-POSS nanocomposites as in the case of EP/POSS, while the particle-to-matrix interactions may be more important in the chemically grafted POSS/polymer nanocomposites, where the POSS molecules are dispersed at the molecular level.

Acknowledgements

This study was supported in part by NSF MSREC (DMR 00880604) and in part by Air Force Research Laboratory. The SAXS synchrotron beamline X27C was supported by Department of Energy (Grant DE-FG02-99ER 45760). We want to express our gratitude to Dr Andy Tsou of ExxonMobil Chemicals and Dr Joseph Lichtenhan of Hybrid Plastics for providing valuable research samples.

References

[1] Lichtenhan JD. Comments Inorg Chem 1995;17:115.
[2] Lichtenhan JD, Noel CJ, Bolf AG, Ruth PN. Mater Res Soc Symp Proc 1996;435:3.
[3] Haddad TS, Lichtenhan JD. Macromolecules 1996;29:7302.
[4] Fu BX, Hsiao BS, Pagola S, Stephens P, White H, Rafailovich M, Mather P, Jeon H, Phillips S, Lichtenhan J, Schwab J. Polymer 2000; 42:599.
[5] Mather PT, Jeon HG, Romo-Uribe A, Haddad TS, Lichtenhan JD. Macromolecules 1998;32:1194.
[6] Lichtenhan JD, Vu NQ, Carter JA, Gilman JW, Feher FJ. Macromolecules 1993;26:2141.
[7] Haddad TS, Lichtenhan JD. J Inorg Organomet Polym 1995;5:237.
[8] Fu BX, Zhang W, Hsiao BS, Rafailovich M, Sokolov J, Johansson G, Sauer B, Phillips S, Blanski R. High Perform Polym 2000;12:565.
[9] Bharadwaj RK, Berry RJ, Farmer BL. Polymer 2000;41:7209.
[10] Fu BX, Yang L, Somani RH, Zong SX, Hsiao BS, Phillips S, Blanski R, Ruth P. J Polym Sci, Polym Phys 2001;39:2727.
[11] Barry AJ, Daudt WH, Domicone JJ, Gilkey JW. J Am Chem Soc 1955;77:4248.
[12] Winter HH, Chambon F. Polym Bull 1985;13:499.
[13] Vilgis TA, Winter HH. Coll Polym Sci 1988;266:494.
[14] Gelfer MY, Winter HH. Macromolecules 1999;32:8974.
[15] Chambon F, Winter HH. J Rheol 1987;31:683.
[16] Winter HH, Chambon F. J Rheol 1986;30:367.
[17] Krishnamoorti R, Giannelis EP. Macromolecules 1997;30:4097.
[18] Chiou B, Raghavan SR, Khan SA. Macromolecules 2001;34:4526.
[19] Munstedt H. Angew Makrom Chem 1975;47:229.
[20] Minagawa N, White JL. Polym Engng Sci 1975;15:825.
[21] Leonov AI. J Rheol 1990;34:1039.
[22] Metzner AB. J Rheol 1985;29:739.
[23] Simhambhatla M, Leonov AI. Rheol Acta 1995;34:329.
[24] Wang MJ, Wolff S. Rubber Chem Tech 1992;65:890.
[25] Romo-Uribe A, Mather PT, Haddad TS, Lichtenhan JD. J Polym Sci, Polym Phys 1998;36:1857.